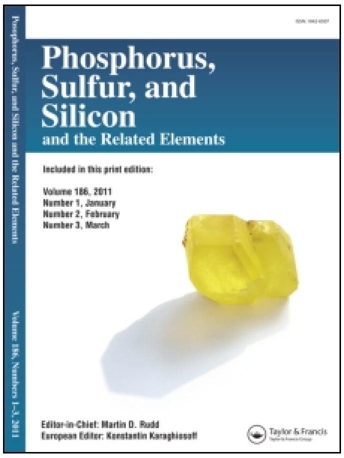

Phosphorus, Sulfur, and Silicon and the Related Elements
Publication details, including instructions for authors and subscription information:
http://www.informaworld.com/smpp/title~content=t713618290

Metal Complexes of Phosphorus Compounds Including Indigoid Structure: Synthesis, Characterization, and Biological Study

Zeinab H. Abd El-Wahab[a]; Abeer A. Faheim[a]
[a] Chemistry Department, Faculty of Science (Girl's), Al-Azhar University, Nasr City, Cairo, Egypt

To cite this Article Abd El-Wahab, Zeinab H. and Faheim, Abeer A.(2009) 'Metal Complexes of Phosphorus Compounds Including Indigoid Structure: Synthesis, Characterization, and Biological Study', Phosphorus, Sulfur, and Silicon and the Related Elements, 184: 2, 341 — 361

To link to this Article: DOI: 10.1080/10426500802145049

URL: http://dx.doi.org/10.1080/10426500802145049

Phosphorus, Sulfur, and Silicon, 184:341–361, 2009

ISSN: 1042-6507 print / 1563-5325 online
DOI: 10.1080/10426500802145049

Metal Complexes of Phosphorus Compounds Including Indigoid Structure: Synthesis, Characterization, and Biological Study

Zeinab H. Abd El-Wahab and Abeer A. Faheim
Chemistry Department, Faculty of Science (Girl's), Al-Azhar University, Nasr City, Cairo, Egypt

*Interaction of hexachlorocyclodiphosph(V)azanes, (I_{a-h}) with 5,5′ indigodisulfonic acid disodium salt (**II**) furnished the expected cyclodiphosph(V)azanes of the type (H_2L^1–H_2L^8). The coordinating behavior of H_2L^1, where H_2L^1 is 1,3diphenyl-2,2,4,4-tetrachloro-2,4-di{1,1′-di(5,5′ indigodisulfonic acid disodium salt)} cyclodiphosph(V)azane, towards the transition metal ions Mn(II), Co(II), Ni(II), Cu(II) and Fe(III) was studied. The structures of the isolated products are proposed based on elemental analyses, molar conductance, spectral analysis (IR, ^{1}H-NMR, and UV-Vis), as well as magnetic susceptibility measurements and thermogravimetric analysis (TGA). From the elemental analyses, 1:2 (ligand:metal) ratio is suggested, and the complexes are found to have the general formula $[(M)_2(L^1)(Cl)_x.n(H_2O)]\cdot zH_2O$ where M = Mn(II) and Co(II) ($x = 2$, $n = 6$, $z = 1$); M = Ni(II) ($x = 2$, $n = 6$, $z = 1.5$); M = Cu(II) ($x = 2$, $n = 2$, z = nil); M = Fe(III) ($x = 4$, $n = 4$, $z = 4$) and (L^1) = the deprotonated form of cyclodiphosphazane ligand. The molar conductance data show that all complexes are non-electrolytes. The spectral data and magnetic susceptibility measurements revealed that the ligand behaves as a dibasic tetradentate ligand coordinated to the metal ions through heterocyclic nitrogen and carbonyl oxygen atoms in an octahedral and square planar manner. Some ligand field parameters (Dq, B, and β), in addition to ligand field stabilization energy (LFSE), were calculated. The thermal behavior of these complexes is studied using TG technique and the different dynamic parameters are calculated applying Coats–Redfern equation. Antimicrobial activities have been studied using the agar–disc diffusion technique, and the higher antimicrobial activity has been observed for the iron (III) complex compared to the other metal complexes.*

Keywords Biological study; cyclodiphosphazane; transition metal complexes

INTRODUCTION

Phosphorus-containing compounds proved to be important in their applications as antioxidants, corrosion resistant material, stabilizers in

---

Received 15 November 2007; accepted 22 April 2008.

Address correspondence to Zeinab A. Abd El-Wahab, Chemistry Department, Faculty of Science (Girl's), Al-Azhar University, P.O. Box, 11754, Nasr City, Cairo, Egypt. E-mail: zhabdelwahab@yahoo.com

plastic manufactures, binders, and coatings in refractory ceramics, oil industry, flam-proofing, and they are used also in phosphate laser glasses as well as agriculture insecticides and fertilizers.[1,2] Interest in the chemistry of phosphorus-containing heterocyclic compounds is linked with their participation in many biochemical processes, with their use as therapeutic preparations and agents for plant protection, and with use in organic synthesis, metal complex catalysis, and other areas.[3] Over the last decade, the ligands based on the cyclodiphosph(III or V)azane framework have been studied because of their ability to coordinate with main group and transition metals.[4,5] Although, the interaction of hexachlorocyclodiphosph(V)azanes with several functional groups containing compounds has been investigated in great detail,[1,2,4,6–16] the literature survey indicates the absence of analogous reactions with 5,5′indigodisulfonic acid disodium salt (indigo carmine). Generally, indigo is one of the earliest known colorants. It was initially extracted from plants and was later marketed as a synthetic product, and it is used mainly for dyeing blue jeans.[17] Indigo carmine is one of the oldest dyes and still one of the most important used. Its major industrial application is the dyeing of clothes (blue jeans) and other blue denim, it has also been employed as redox indicator in analytical chemistry and as a microscopic stain in biology, and additionally it has been used as a food additive and as a diagnostic drug.[18–20]

The main aim of this work and in continuance of our work on the coordination chemistry of cyclodiphosph(V)azanes, is to design novel multidentate cyclic phosphorus–nitrogen ligands that are multifunctional systems particularly capable of holding two metal ions. So we describe here the synthesis and structural characterization of cyclodiphosph(V)azanes (**H_2L^1–H_2L^8**) including indigoid structure followed by studying the complexation behavior toward Mn(II), Co(II), Ni(II), Cu(II), and Fe(III) ions via different physicochemical tools such as elemental analysis, molar conductance, magnetic moment, spectral (IR,^{1}H-NMR and UV-Vis), and thermal analyses. Furthermore, the synthesized compounds were screened for their antimicrobial activity in an attempt to understand the influence of metal ion and the ligand nature on the biological properties.

EXPERIMENTAL

Analysis and Physical Measurements

All chemicals used were of highest available purity. They include $MnCl_2{\cdot}4H_2O$, $CoCl_2{\cdot}6H_2O$, $NiCl_2{\cdot}6H_2O$, $CuCl_2{\cdot}2H_2O$, and $FeCl_3{\cdot}6H_2O$ (BDH or Sigma); 5,5′indigodisulfonic acid disodium salt (indigo carmine) and phosphorus pentachloride (Aldrich); and aryl amines: aniline, p-toluidine, o- and p-anisidine, o- and p-nitroaniline, and o- and p-chloroaniline (BDH, Sigma and Aldrich). Organic solvents used included absolute ethyl alcohol, benzene, acetonitrile, diethylether, dimethylformamide (DMF), and dimethylsulfoxide (DMSO), which were purchased from Merck or Sigma. Concentrated nitric and perchloric acid were reagent grade and were used as supplied.

Carbon, hydrogen, nitrogen, and sulfur contents were determined using a Perkin-Elmer 2408 CHN analyzer. Metal contents were determined by titration against standard EDTA solution after complete decomposition of the complexes and the chloride and phosphorus contents were determined gravimetrically.[21] Melting or decomposition points were carried out on a melting point apparatus, Gallenkamp, England. IR spectra were recorded on a Perkin-Elmer FT-IR type 1650 spectrophotometer using KBr discs. ^{1}H-NMR spectra were recorded using a Brucker ARX-300 spectrometer using DMSO-d$_6$ as a solvent. Electronic spectra of the ligands and the metal complexes were recorded on a Jasco model V-550 UV-vis spectrophotometer. Magnetic susceptibility of the metal complexes were measured by the Gouy method at room temperature using a Johnson Matthey, Alpha products, model MKI magnetic susceptibility balance, and the effective magnetic moments were calculated using the relation $\mu_{\text{eff}} = 2.828\ (\chi_{\text{m}}.\text{T})^{1/2}$ B.M, where χ_{m} is the molar susceptibility corrected using Pascal's constants for diamagnetism of all atoms in the compounds. The molar conductance measurements were measured in solutions of the metal complexes in DMF (10^{-3}M) using a WTWD-812 Weilheium-Conductivity meter model LBR, fitted with a cell model LTA100. A Shimadzu TGA-50H thermal analyzer was used to record simultaneously the thermogravimetric (TG) and differential thermogravimetric (DTG) curves, the experiments were carried out in dynamic nitrogen atmosphere (20 mL min^{-1}) with a heating rate 10°C min^{-1} within the temperature range from room temperature up to 1000°C using platinum crucibles. Highly sintered α-Al$_2$O$_3$ was used as a reference. Additionally, the antimicrobial activity was done using the agar–disc diffusion technique.[22]

Synthesis of Cyclodiphosph(V)azanes (H_2L^1–H_2L^8)

The cyclodiphosph(V)azanes, (**H_2L^1–H_2L^8**) were prepared through two steps. The first step was preparation of hexachlorocyclodiphosph(V)azanes (**I_{a-h}**) using the methods of Chapmann and Kirsanov. A solution of aryl amine (0.1 mol) in 80 mL cold, dry benzene was added in small portions to a stirred cold solution of phosphorus pentachloride (0.1 mol) in 100 mL cold, dry benzene during half hour at 15°C. After the addition was completed, the reaction mixture was heated under reflux for 3 h under anhydrous conditions with continuous stirring. After the completion of the reaction (HCl gas ceased to evolve), the reaction mixture was cooled to room temperature, and the solids obtained were filtered then washed several times with dry benzene and dry diethylether to give 1,3diaryl-2,2,2,4,4,4-hexachlorocyclodiphosph(V)azanes ($\mathbf{I_{a-h}}$). The second step was the addition of 5,5′indigodisulfonic acid disodium salt (**II**) (0.2 mol) in 80 mL cold, dry acetonitrile in small portions to a stirred cold solution of the prepared cyclodiphosph(V)azanes ($\mathbf{I_{a-h}}$) (0.1 mol) in 100 mL cold, dry acetonitrile during a half-hour at 15°C. After the addition was completed, the reaction mixture was heated under reflux for 7 h under anhydrous conditions with continuous stirring, then the solids obtained were filtered and washed several times with dry acetonitrile and dry diethylether to give 1,3diaryl-2,2,4,4-tetrachloro-2,4-di{1,1′‘-{di(5,5′indigodisulfonic acid disodium salt)} cyclodiphosph(V)azanes ($\mathbf{H_2L^1}$–$\mathbf{H_2L^8}$). These products are of importance because of the presence of several reactive sites that make them highly reactive and susceptible to undergo a variety of functionalization processes. Figure 1 illustrates the synthetic scheme of cyclodiphosph(V)azanes ($\mathbf{H_2L^1}$–$\mathbf{H_2L^8}$). Their elemental analysis and some physicochemical characteristic data are collected in Table I.

Synthesis of Metal Complexes

A solution of respective metal chloride, namely, $MnCl_2{\cdot}4H_2O$, $CoCl_2{\cdot}6H_2O$, $NiCl_2{\cdot}6H_2O$, $CuCl_2{\cdot}2H_2O$, or $FeCl_3{\cdot}6H_2O$, dissolved in ethanol (40 mL) was added dropwise to a stirred ethanolic solution of 1,3diphenyl-2,2,4,4-tetrachloro-2,4-di{1,1′-di (5,5′indigodisulfonic acid disodium salt)} cyclodiphosph(V)azane ($\mathbf{H_2L^1}$) (60 mL) in a 2:1 metal-to-ligand molar ratio at room temperature with continuous stirring. After complete addition of the metal–salt solution, the reaction mixture was heated under reflux with continuous stirring for 3 h to ensure the complete precipitation of the formed complexes. The precipitated solid complexes were filtered, washed several times with ethanol followed by diethylether, and dried in a vacuum desiccator over anhydrous calcium chloride. All metal complexes (**1–5**) are received as powder, stable in air, insoluble in common organic solvents but soluble in DMF and DMSO, and give elemental analysis consistent with the proposed structures. Their elemental analysis and some physicochemical characteristic data are collected in Table II.

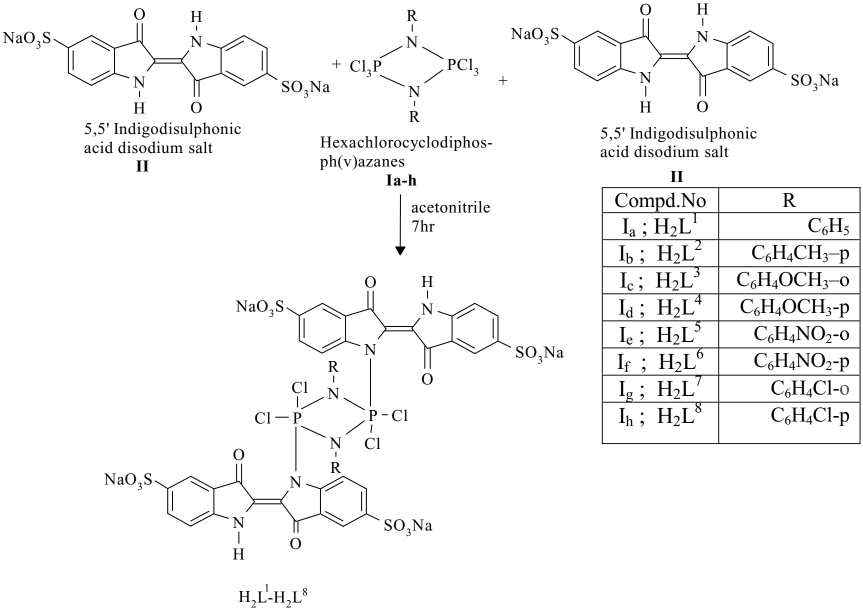

Compd.No	R
I_a ; H_2L^1	C_6H_5
I_b ; H_2L^2	$C_6H_4CH_3$–p
I_c ; H_2L^3	$C_6H_4OCH_3$–o
I_d ; H_2L^4	$C_6H_4OCH_3$-p
I_e ; H_2L^5	$C_6H_4NO_2$-o
I_f ; H_2L^6	$C_6H_4NO_2$-p
I_g ; H_2L^7	C_6H_4Cl-o
I_h ; H_2L^8	C_6H_4Cl-p

FIGURE 1 Schematic diagram for preparation of cyclodiphosph(v)azanes, (H_2L^1–H_2L^8). H_2L^1: 1,3diphenyl-2,2,4,4-tetrachloro-2,4-di{1,1′-di(5,5′indigodisulfonic acid disodium salt)} cyclodiphosph (V)azane. H_2L^2: 1,3di(p-tolyl)-2,2,4,4-tetrachloro-2,4-di{1,1′-di(5,5′indigodisulfonic acid disodium salt)} cyclodiphosph(V)azane. H_2L^3: 1,3di(o-anisidyl)-2,2,4,4-tetrachloro-2,4-di{1,1′-di(5,5′indigodisulfonic acid disodium salt)} cyclodiphosph(V)azane. H_2L^4: 1,3di (p-anisidyl)-2,2,4,4-tetrachloro-2,4-di{1,1′-di(5,5′indigodisulfonic acid disodium salt)} cyclodiphosph(V)azane. H_2L^5: 1,3di(o-nitrophenyl)-2,2,4,4-tetrachloro-2,4-di{1,1′-di(5,5′indigodisulfonic acid disodium salt)} cyclodiphosph (V)azane. H_2L^6: 1,3di(p-nitrophenyl)-2,2,4,4-tetrachloro-2,4-di{1,1′-di(5,5′ indigodisulfonic acid disodium salt)} cyclodiphosph(V)azane. H_2L^7: 1,3di(o-chlorophenyl)-2,2,4,4-tetrachloro-2,4-di{1,1′-di(5,5′indigodisulfonic acid disodium salt)} cyclodiphosph(V)azane. H_2L^8: 1,3di(p-chlorophenyl)-2,2,4,4-tetrachloro-2,4-di{1,1′-di(5,5′indigodisulfonic acid disodium salt)} cyclodiphosph(V)azane

Antimicrobial Assay

The cyclodiphosph(V)azane ligand (**H_2L^1**) and its metal complexes (**1**–**5**) in addition to $MnCl_2 \cdot 4H_2O$, $CoCl_2 \cdot 6H_2O$, $NiCl_2 \cdot 6H_2O$, $CuCl_2 \cdot 2H_2O$, and $FeCl_3 \cdot 6H_2O$ were screened for antibacterial and antifungal activity against the sensitive organisms *Staphylococcus aureus* (ATCC 25923) and *Streptococcus pyogenes* (ATCC 19615) as Gram-positive bacteria,

TABLE I Characterization Data of Cyclodiphosph(V)azanes (H_2L^1–H_2L^8)

Compd. No. Empirical formula	Color	M.P. (°C)	Elemental analysis, found (calcd. %)					
			C	H	N	P	Cl	S
H_2L^1; $C_{44}H_{24}N_6P_2O_{16}Cl_4S_4Na_4$	Pale blue	182	40.00	1.47	6.34	4.03	10.25	9.72
(1316.72)			(40.13)	(1.84)	(6.38)	(4.70)	(10.77)	(9.74)
H_2L^2; $C_{46}H_{28}N_6P_2O_{16}Cl_4S_4Na_4$	Dark blue	289	41.00	2.00	6.81	4.06	11.00	9.58
(1344.78)			(41.08)	(2.10)	(6.25)	(4.61)	(10.54)	(9.54)
H_2L^3; $C_{46}H_{28}N_6P_2O_{18}Cl_4S_4Na_4$	Sky blue	257	39.79	2.37	6.69	4.97	11.04	9.39
(1376.78)			(40.13)	(2.05)	(6.11)	(4.50)	(10.30)	(9.32)
H_2L^4; $C_{46}H_{28}N_6P_2O_{18}Cl_4S_4Na_4$	Faint blue	290	40.54	1.99	6.33	4.20	10.46	8.98
(1376.78)			(40.13)	(2.05)	(6.11)	(4.50)	(10.30)	(9.32)
H_2L^5; $C_{44}H_{22}N_8P_2O_{20}Cl_4S_4Na_4$	Dark blue	155	38.00	1.94	7.61	4.43	10.05	9.74
(1406.72)			(37.57)	(1.58)	(7.97)	(4.40)	(10.08)	(9.12)
H_2L^6; $C_{44}H_{22}N_8P_2O_{20}Cl_4S_4Na_4$	Pale blue	242	38.09	1.90	7.37	4.82	14.92	8.97
(1406.72)			(37.57)	(1.58)	(7.97)	(4.40)	(10.08)	(9.12)
H_2L^7; $C_{44}H_{22}N_6P_2O_{16}Cl_6S_4Na_4$	Sky blue	269	38.36	1.77	5.99	4.65	14.92	9.01
(1385.60)			(38.14)	(1.60)	(6.07)	(4.47)	(15.35)	(9.26)
H_2L^8; $C_{44}H_{22}N_6P_2O_{16}Cl_6S_4Na_4$	Pale blue	241	38.99	1.91	6.38	4.85	14.99	8.96
(1385.60)			(38.14)	(1.60)	(6.07)	(4.47)	(15.35)	(9.26)

TABLE II Characterization Data of Metal Complexes 1–5

Compd. No.[a] Empirical formula	Color	M.P. (°C)	Λ_m^b	$\mu_{eff.}$ (BM)[c]	Elemental analysis, found (calcd. %)						
					C	H	N	P	Cl	S	M
(1); $[(Mn)_2(L^1)(Cl)_2(H_2O)_6] \cdot H_2O$	Pale blue	290	9.00	5.50	32.00	1.27	5.34	3.31	13.25	8.01	6.92
$Mn_2C_{44}H_{22}N_6P_2O_{16}Cl_6S_4Na_4.7H_2O$ (1621.62)					(32.59)	(1.37)	(5.18)	(3.82)	(13.12)	(7.91)	(6.78)
(2); $[(Co)_2(L^1)(Cl)_2(H_2O)_6] \cdot H_2O$	Bluish green	>300	10.28	4.89	32.09	1.33	5.81	3.27	13.38	7.35	7.05
$Co_2C_{44}H_{22}N_6P_2O_{16}Cl_6S_4Na_4.7H_2O$ (1629.60)					(32.43)	(1.36)	(5.16)	(3.80)	(13.05)	(7.87)	(7.20)
(3); $[(Ni)_2(L^1)(Cl)_2(H_2O)_6] \cdot 1\frac{1}{2}H_2O$	Bluish green	287	11.35	3.02	32.92	1.27	5.69	3.09	12.64	7.24	7.36
$Ni_2C_{44}H_{22}N_6P_2O_{16}Cl_6S_4Na_4.7\frac{1}{2}H_2O$ (1638.13)					(32.26)	(1.36)	(5.13)	(3.78)	(12.98)	(7.83)	(7.17)
(4); $[(Cu)_2(L^1)(Cl)_2(H_2O)_2]$	Bluish green	296	8.75	1.98	34.54	1.70	15.33	3.88	13.46	8.09	8.28
$Cu_2C_{44}H_{22}N_6P_2O_{16}Cl_6S_4Na_4.2H_2O$ (1548.74)					(34.12)	(1.43)	(5.43)	(4.00)	(13.73)	(8.28)	(8.21)
(5); $[(Fe)_2(L^1)(Cl)_4(H_2O)_4] \cdot 4H_2O$	Dark blue	279	7.44	5.91	30.33	1.39	4.61	3.39	16.05	7.08	6.03
$Fe_2C_{44}H_{22}N_6P_2O_{16}Cl_8S_4Na_4.8H_2O$ (1712.36)					(30.86)	(1.30)	(4.91)	(3.62)	(16.56)	(7.49)	(6.52)

[a] **1–5** represent cyclodiphosph(V)azane metal complexes; L^1 represent the deprotonated form of the cyclodiphosph(V)azane ligand H_2L^1.

[b] Molar conductance (ohm^{-1} cm^2 mol^{-1}) of 1×10^{-3} M solution in DMF at room temperature.

[c] Room temperature effective magnetic moment for each metal ion.

Pseudomonas phaseolicola (GSPB 2828) and *Pseudomonas fluorescens* (S 97) as Gram-negative bacteria, and the fungi *Fusarium oxysporum*, *Aspergillus fumigatus*, and *Candida albicans*. The antibiotics Cephalothin, Chloramphencol, and Cycloheximide were used as standard references for Gram-positive bacteria, Gram-negative bacteria, and fungi, respectively, using the agar–disc diffusion technique[22] described below:

The tested compounds were dissolved in DMF, which has no inhibition activity to get concentrations of 6.46×10^{-4} to 5.87×10^{-3} M/L. The test was performed on medium potato dextrose agar (PDA), which contains an infusion of 200 g potatoes, 6 g dextrose, and 15 g agar. Uniform size filter paper disks (3 disks per compound) were impregnated by an equal volume (10 μl) from the specific concentration of dissolved tested compounds and carefully placed on inoculated agar surface. After incubation for 36 h at 27°C in the case of bacteria and for 48 h at 24°C in the case of fungi, inhibition of the organisms, which was evidenced by a clear zone surround each disk, was measured and used to calculate the mean of inhibition zones.

RESULTS AND DISCUSSION

In the present investigation, phosphorus pentachloride reacted in cold, dry benzene with aryl amines (1:1 molar ratio) to give 1,3diaryl-2,2,2,4,4,4-hexa-chlorocyclodiphosph(V)azanes ($\mathbf{I_{a-h}}$). The interaction between these products and 5,5′indigodisulfonic acid disodium salt (**II**) in acetonitrile solution (1:2 molar ratio, respectively) led to cyclosubstitution at the phosphorus atom by the elimination of one chlorine atom from each side as HCl gas furnishing 1,3diaryl-2,2,4,4-tetrachloro-2,4-di{1,1′-{di (5,5′indigodisulfonic acid disodium salt)} cyclodiphosph(V)azanes ($\mathbf{H_2L^1}$-$\mathbf{H_2L^8}$).

Because the cyclodiphosph(V)azanes, ($\mathbf{H_2L^1}$-$\mathbf{H_2L^8}$) have similar structures, the ligand; 1,3diphenyl-2,2,4,4-tetrachloro-2,4-di{1,1′-{di(5,5′indigodisulfonic acid disodium salt)} cyclodiphosph(V)azane ($\mathbf{H_2L^1}$) was selected to study their behavior towards some metal ions such as Mn (II), Co(II), Ni(II), Cu(II), and Fe(III), which is the our goal in this article. The isolated metal complexes (**1**–**5**) gave elemental analysis (Table II) compatible with the suggested formula in which the ligand-metal stoichiometry for all complexes is 1:2, respectively. The assignment of the proposed structures for the isolated compounds is based on the different physicochemical tools.

Characterization of Cyclodiphosph(V)azanes (H_2L^1–H_2L^8)

The assignment of the proposed structure for 1,3diaryl-2,2,4,4-tetrachloro-2,4-di{1,1′-{di(5,5′-indigodisulfonic acid disodium salt)} cyclodiphosph(V)azanes (**H_2L^1–H_2L^8**) is based on the following:

1. The elemental analyses data (Table I) are compatible with the suggested structure.
2. The UV spectra in DMF solvent showed absorption bands at 277–288 nm (36,101–34,722 cm^{-1}), which are characteristic for the electron delocalization within the phosphazo four-membered rings.[8]
3. The ^{1}H-NMR spectra (Table III) showed the characteristic proton signals at δ 10.65–10.64 ppm (s, NH), δ 7.76–6.41 ppm (m, phenyl protons), δ 3.60 ppm (s, OCH_3), and δ 2.56 ppm (s, CH_3).[8]
4. The infrared spectra (Table III) showed the characteristic bands in the spectral range of 3300–3290 cm^{-1}; 1660–1658 $cm^{-1}$and 1628–1610 cm^{-1}; 1490–1470 cm^{-1}; 1025–1010 cm^{-1}; and 600–579 cm^{-1} that can be reasonably assigned to ν(N—H), ν(C=O), ν(C=C), ν(P—N), and ν(P-Cl), respectively.[4,7,17,23]

TABLE III Main IR and ^{1}H-NMR Data with Their Assignment for Cyclodiphosph(V)azanes (H_2L^1–H_2L^8)

	IR bands (cm^{-1})					
Compd. No.	ν_{N-H}	$\nu_{C=O}$	$\nu_{C=C}$	ν_{P-N}	ν_{P-Cl}	^{1}H-NMR (δ, ppm)
H_2L^1	3300	1660, 1628	1475	1025	600	10.64 (s, NH), 7.76–6.52 (m, phenyl proton)
H_2L^2	3290	1662, 1614	1470	1010	600	10.65 (s, NH), 7.75–6.41 (m, phenyl proton), 2.56 (s,CH_3)
H_2L^3	3290	1668, 1615	1475	1025	588	10.64 (s, NH), 7.65–6.71 (m, phenyl proton), 3.60 (s,OCH_3)
H_2L^4	3296	1660, 1610	1480	1022	579	10.64 (s, NH), 7.76–6.48 (m, phenyl proton), 3.60 (s,OCH_3)
H_2L^5	3300	1659, 1620	1490	1020	590	10.64 (s, NH), 7.65–6.71 (m, phenyl proton)
H_2L^6	3298	1664, 1622	1480	1010	580	10.64 (s, NH), 7.66–6.56 (m, phenyl proton)
H_2L^7	3294	1660, 1619	1475	1022	588	10.64 (s, NH), 7.75–6.75 (m, phenyl proton)
H_2L^8	3300	1658, 1621	1470	1025	580	10.64 (s, NH), 7.76–6.52 (m, phenyl proton)

s, singlet; m, multiplet.

Characterization of Metal Complexes (1–5)

The chemical behavior of cyclodiphosph(V)azane ligand (**H_2L^1**) towards the transition metal cations was the our goal in this article. The metal cations selected for this purpose were Mn(II), Co(II), Ni(II), Cu(II), and Fe(III). When a mixture of one mole of cyclodiphosph(V)azane ligand (**H_2L^1**) in dry ethanol was reacted with two moles of the metal salts in dry ethanol, the metal complexes (**1**–**5**) were obtained and gave elemental analysis compatible with the suggested formula. Accordingly, the metal complexes are prepared following the general equation:

$$H_2L^1 + 2MCl_x \cdot nH_2O \rightarrow [(M)_2L^1(Cl)_y \cdot m(H_2O)]Z + 2\ HCl$$

$$M = Mn(II) : x = 2,\ n = 4,\ y = 2,\ m = 6,\ z = H_2O$$

$$Co(II) : x = 2,\ n = 6,\ y = 2,\ m = 6,\ z = H_2O$$

$$Ni(II) : x = 2,\ n = 6,\ y = 2,\ m = 6,\ z = 1.5\ H_2O$$

$$Cu(II) : x = 2,\ n = 2,\ y = 2,\ m = 2,\ z = nil$$

$$Fe(III) : x = 3,\ n = 6,\ y = 4,\ m = 4,\ z = 4H_2O$$

The proposed composition of the metal complexes is confirmed using the different physicochemical tools. For the structures, see the following four sections. Additionally, the biological activity was done.

Conductivity Measurements

The molar conductance data of the metal complexes (**1**–**5**) at room temperature in 10^{-3}M DMF solutions were found to be in the range 11.35–7.44 $ohm^{-1}cm^2\ mol^{-1}$. Table II revealed the non-electrolytic nature of these complexes. This can be accounted for by the satisfaction of the bi- or trivalency of the metal by the chloride anion. This implies the coordination of the anions to the metal ion centers.[1,24]

IR Spectra

A comparative study of the IR spectra of the metal complexes with that of the free ligand and those of the complexes of related ligands gives some positive information regarding the binding sites of the cyclodiphosph(V)azanes.

The IR spectra of metal complexes (Table IV) show that the stretching vibration band ν(NH) of heterocyclic ring (which in the free ligand, **H_2L^1** at 3300 cm^{-1}) disappeared in the spectra of all metal complexes (**1**–**5**) indicating the deprotonation of this group as a result of complexation with metal ions. The strong absorption band appearing in the IR spectrum of the free ligand **H_2L^1** at 1628 cm^{-1} assigned to

TABLE IV Characteristic IR Bands for Cyclodiphosph(V)azane, (H_2L^1) and Its Metal Complexes 1–5

	IR bands (cm^{-1})							
Compd. No.	ν_{O-H} (H_2O)	ν_{N-H}	$\nu_{C=O}$	$\nu_{C=C}$	ν_{P-N}	ν_{P-Cl}	ν_{M-O}	ν_{M-N}
H_2L^1	—	3300	1660, 1628	1475	1025	600	—	—
1	3410	—	1658, 1615	1474	1023	600	525	490
2	3492	—	1659, 1600	1473	1025	598	500	440
3	3400	—	1660, 1620	1471	1024	600	501	420
4	3420	—	1658, 1620	1475	1025	598	535	480
5	3428	—	1658, 1600	1473	1023	600	510	460

theν(C=O) stretching vibrations appears at lower wave numbers (1620–1600 cm^{-1}) in all metal complexes in accordance with the coordination of this group in complex formation, while there is little change for the other carbonyl group (1660–1658 cm^{-1}), thus ruling out its coordination. Conclusive evidence regarding the bonding of both heterocyclic nitrogen and carbonyl oxygen atoms to the metal ions is provided by the appearance of new medium and/or weak bands at lower frequencies between 535–500 cm^{-1} and 490–420 cm^{-1} as a result of ν(M—O) and ν(M—N) stretching modes, respectively.[4,25] These stretches were not present in the spectra of the free ligand. The broad bands observed at 3492–3400 cm^{-1} in the spectra of all metal complexes can be assigned to the presence of water and/or coordinated water molecules[25] supported by thermal analyses (see Kinetic Study section). It is obvious from the IR data that cyclodiphosph(V)azane ligand, (**H_2L^1**) behaves as a dibasic tetradentate ligand coordinated to the metal ions through the deprotonated heterocyclic nitrogen and carbonyl oxygen atoms.

Magnetic Properties and Electronic Spectra

The magnetic moments of the metal complexes are measured at room temperature and given in Table II. The complexes show magnetic moment values of 5.50 and 5.91 BM corresponding to five unpaired electrons expected for Mn(II) and Fe(III) complexes; 4.89, 3.02, and 1.98 BM corresponding to three, two, and one unpaired electrons expected for Co(II), Ni (II), and Cu(II) complexes, respectively.[26]

The electronic spectra of the metal complexes showed absorption bands at 270–283 nm (37,037–35,336 cm^{-1}), which are characteristic of the phosphazo four-membered ring.[8] The reflectance spectra of Mn(II) and Fe(III) complexes **1** and **5** display one weak band at 23,474 cm^{-1} for Mn(II) complex (**1**) and 21,186 cm^{-1} for Fe(III) complex (**5**). These may be assigned to the charge transfer band L→M in addition to two bands at 15,552 and 17,857 cm^{-1} for Mn(II) complex (**1**) and 16,807, 17,730 cm^{-1} for Fe(III) complex (**5**), which may be assigned to $^6A_{1g} \rightarrow {}^4T_{1g}$ transition. These results, together with the measured magnetic moments values, are compatible with those reported for octahedral geometry around Mn(II) and Fe(III) ions. The electronic spectrum of cobalt (II) complex (**2**) displays two absorption bands at 17,036 and 19,231 cm^{-1} may be assignable to $^4T_{1g}$ (F) $\rightarrow {}^4A_{2g}$ (F) and $^4T_{1g}$ (F) $\rightarrow {}^4T_{1g}$ (P) transitions, respectively, suggesting octahedral configuration. The value of magnetic moment (4.89 BM) is in good agreement with those reported for the octahedral structure. The electronic spectrum of nickel (II) complex (**3**) displays three absorption bands at 12,853, 19,802, and 20,325 cm^{-1}, suggesting octahedral configuration about Ni (II) ion and may attributed to $^3A_{2g}(F) \rightarrow {}^3T_{2g}(F)$, $^3A_{2g}(F) \rightarrow {}^3T_{1g}(F)$, and $^3A_{2g}(F) \rightarrow {}^3T_{1g}$ (P) transitions, respectively. The magnetic moment value (3.02 BM) is in good agreement with those reported for the octahedral structure. The electronic spectrum of copper (II) complex (**4**) gave two bands at 14,577 and 16,287 cm^{-1} which may be assignable to the transition $^2B_{1g} \rightarrow {}^2B_{2g}$ and $^2B_{1g} \rightarrow {}^2E_g$, suggesting square planar geometry. Its magnetic moment value (1.98 BM) supports the square planar structure. The data that characterize these metal complexes are analogous to other metal complexes containing a phosphazo four-membered ring.[4,6,27,28]

Various ligand field parameters, (D_q, B, and β) in addition to ligand field stabilization energy (LFSE) were calculated for octahedral Co(II) and Ni(II) complexes (Table V). In the octahedral cobalt complex, the values of (υ_2) and (υ_3) are used to calculate the parameters (10 D_q) and (B), while in the octahedral Ni (II) complex, the energy of the first spin allowed transition directly and gives the value of (10D_q); also (B) values have been calculated.[29]

Thermogravimetric Study

The thermogravimetric study for the metal complexes was carried out within the temperature range from room temperature up to 1000°C. The determined temperature ranges and percent losses in mass of the solid complexes on heating are given in Table VI. The results obtained are in good agreement with the theoretical formulae suggested from the elemental analyses. Different thermodynamic parameters are calculated and listed in Table VII. Details are provided for the complex $[(Mn)_2L^1(Cl)_2(H_2O)_6]\cdot H_2O$. Figure 2 shows a representative example for thermal analysis of the metal complexes under study, and reveals the following findings:

TABLE V Electronic Parameters Data of Co(II) and Ni(II) Metal Complexes*

Compd. No.	Suggested structure	Absorption bands (nm)/peak assignment			Dq (cm^{-1})	B (cm^{-1})	β	β%	LFSE (cm^{-1})
		υ_1	υ_2	υ_3					
2	octahedral		17036 $^4T_{1g}(F) \rightarrow {}^4A_{2g}(F)$	19231 $^4T_{1g}(F) \rightarrow {}^4T_{1g}(P)$	907	825	0.74	26.34	7258
3	octahedral	12853 $^3A_{2g}(F) \rightarrow {}^3T_{2g}(F)$	19802 $^3A_{2g}(F) \rightarrow {}^3T_{1g}(F)$	20325 $^3A_{2g}(F) \rightarrow {}^3T_{1g}(P)$	1285	821	0.76	23.98	15424

*The ligand field splitting energy (*Dq*), interelectronic repulsion parameter (*B*), nephelauxetic ratio (β), and ligand field stabilization energy (LFSE). The lowering in the *B* values compared to the free metal ion values (1120 and 1080 for Co(II) and Ni(II) ions, respectively) suggests an appreciable amount of covalent character in the metal–ligand bonds. Additionally, the β value is less than unity suggesting a largely covalent bond between the organic ligand and metal (II) ions in these complexes.

TABLE VI Thermoanalytical Results of Metal Complexes

		Temp.	Mass loss%			
Complex compound	Stage	range (°C)	Calcd.	Found	Evolved moiety	Residue
1 $[(Mn)_2L^1(Cl)_2(H_2O)_6]\cdot H_2O$	I	43–86	1.11	1.31	H_2O (hydr.)	$[(Mn)_2L^1(Cl)_2(H_2O)_6]$
	II	86–152	2.22	2.48	H_2O (coord.)	$[(Mn)_2L^1(Cl)_2(H_2O)_5]$
	III	152–253	4.44	5.04	2 H_2O (coord.)	$[(Mn)_2L^1(Cl)_2(H_2O)_3]$
	IV	253–350	12.15	12.00	3 H_2O (coord.) and Cl_2	$[(Mn)_2L^1]$
	V	350–795	64.98	65.00	Decomposition of organic molecule	$2MnCl_2$, $2Na_2S_2O_3$
2 $[(Co)_2L^1(Cl)_2(H_2O)_6]\cdot H_2O$	I	43–257	4.42	4.94	H_2O (hydr.) and 3 H_2O (coord.)	$[(Co)_2L^1(Cl)_2(H_2O)_3]$
	II	257–365	12.09	12.00	3 H_2O (coord.) and Cl_2	$[(Co)_2L^1]$
	III	365–788	64.66	65.00	Decomposition of organic molecule	2 $CoCl_2$, $2Na_2S_2O_3$
3 $[(Ni)_2L^1(Cl)_2(H_2O)_6]\cdot 1\frac{1}{2}H_2O$	I	45–92	1.65	2.47	$1\frac{1}{2}H_2O$ (hydr.)	$[(Ni)_2L^1(Cl)_2(H_2O)_6]$
	II	92–184	3.85	4.69	2 H_2O (coord.)	$[(Ni)_2L^1(Cl)_2(H_2O)_4]$
	III	184–300	12.58	12.80	4 H_2O (coord.) and Cl_2	$[(Ni)_2L^1]$
	IV	300–580	32.64	32.80	$\frac{1}{4}L^1$	$[(Ni)_2, \frac{3}{3}L^1]$
	V	580–793	64.87	65.00	Decomposition of organic molecule	2 $NiCl_2$, $2Na_2S_2O_3$
4 $[(Cu)_2L^1(Cl)_2(H_2O)_2]$	I	150–338	2.33	2.40	2 H_2O (coord.)	$[(Cu)_2L^1(Cl)_2]$
	II	338–427	6.91	7.20	Cl_2	$[(Cu)_2L^1]$
	III	427–519	28.13	28.00	$\frac{1}{4}L^1$	$[(Cu)_2.\frac{3}{3}L^1]$
	IV	519–779	85.86	86.40	Decomposition of organic molecule	2Cu.4Na
5 $[(Fe)_2L^1(Cl)_4(H_2O)_4]\cdot 4H_2O$	I	38–118	4.21	4.98	4 H_2O (hydr.)	$[(Fe)_2L^1(Cl)_4(H_2O)_4]$
	II	118–230	8.42	8.00	4 H_2O (coord.)	$[(Fe)_2L^1(Cl)_4]$
	III	230–496	35.90	36.00	2 Cl_2 and $\frac{1}{4}$ L^1	$[(Fe)_2.\frac{3}{3}L^1]$
	IV	496–757	88.11	87.20	Decomposition of organic molecule	2 Fe.4Na

TABLE VII Thermodynamic Data of the Thermal Decomposition Steps of Metal Complexes

Complex compound	Stage	E* (kJ mol^{-1})	ΔS* (JK^{-1} mol^{-1})	ΔH* (kJ mol^{-1})	ΔG* (kJ mol^{-1})
1 $[(Mn)_2L^1(Cl)_2(H_2O)_6]\cdot H_2O$	I	38.24	−88.12	35.43	29.82
	II	55.18	−65.99	51.92	25.92
	III	76.99	−66.80	73.03	22.75
	IV	99.27	−70.41	94.49	40.58
	V	143.02	−48.97	135.98	57.77
2 $[(Co)_2L^1(Cl)_2(H_2O)_6]\cdot H_2O$	I	36.55	−94.05	33.03	39.82
	II	65.59	−43.90	60.73	25.70
	III	102.27	−29.32	95.20	57.57
3 $[(Ni)_2L^1(Cl)_2(H_2O)_6]\cdot 1\frac{1}{2}H_2O$	I	44.35	−100.39	41.51	34.37
	II	66.98	−46.33	63.56	19.11
	III	88.79	−83.26	84.51	42.96
	IV	113.65	−46.90	107.72	33.55
	V	155.39	−67.70	147.41	65.14
4 $[(Cu)_2L^1(Cl)_2(H_2O)_2]$	I	60.94	−47.39	56.64	24.56
	II	104.38	−26.81	98.93	17.69
	III	179.04	−30.62	172.84	23.02
	IV	214.83	−57.62	202.16	53.33
5 $[(Fe)_2L^1(Cl)_4(H_2O)_4]\cdot 4H_2O$	I	59.21	−39.79	56.29	14.02
	II	89.67	−81.91	85.95	36.70
	III	112.58	−46.40	107.29	29.62
	IV	139.91	−68.83	132.43	62.08

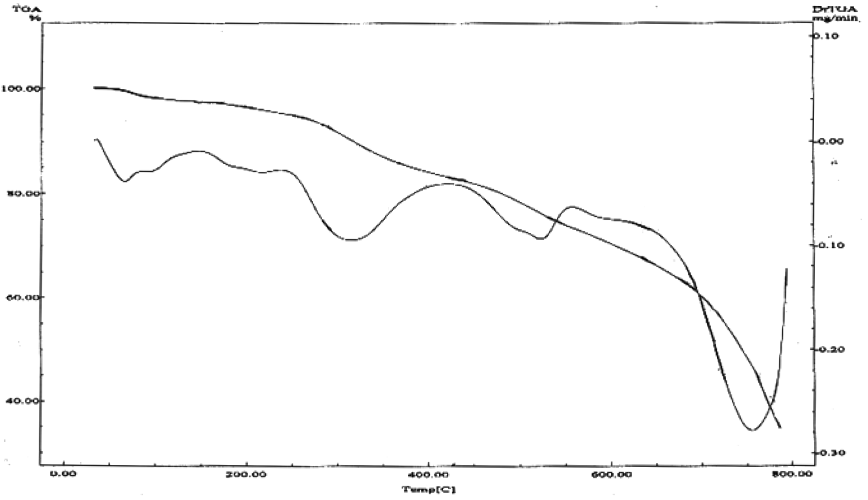

FIGURE 2 TG thermograms for metal complex $[(Mn)_2L^1(Cl)_2(H_2O)_6]\cdot H_2O$.

The first decomposition stage takes place at temperature range 43–86°C, corresponding to release of one molecule of H_2O (hydrated). This step brings weight loss of 1.31% against the calculated loss of 1.11%. The second decomposition stage occurs at 86–152°C, and the mass loss observed is 2.48% against the calculated loss of 2.22%, which may arise from the elimination of one molecule of H_2O (coordinated). The third stage of decomposition occurs at 152–253°C, and the mass loss observed is 5.04% against a calculated loss of 4.44% due to a loss of two molecules of H_2O (coordinated). The fourth stage of decomposition occurs in the 253–350°C range, and the mass loss observed is 12.00% against a calculated loss of 12.15%, corresponding to loss of three molecules of H_2O (coordinated) and Cl_2. The final stage of decomposition is two steps within the temperature range 350–795°C, which represents the decomposition of the organic part with a found mass loss of 65.00% (calcd.64.98%). At the end of the thermogram, $2MnCl_2{\cdot}2Na_2S_2O_3$was the residue [calculated (found) %: 35.02 (35.00)]. The thermal decomposition is suggested to proceed as shown in Scheme 1:

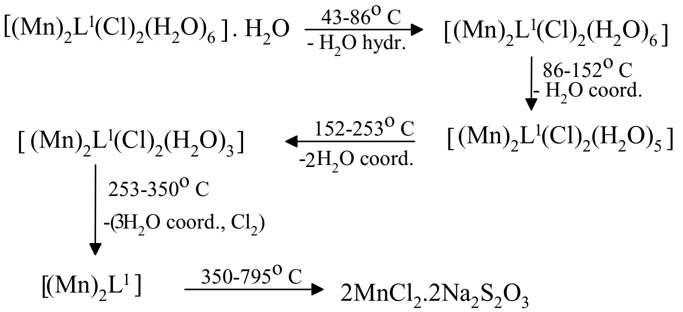

SCHEME 1

The thermal decomposition for the other metal complexes is summarized in Schemes 2–5:

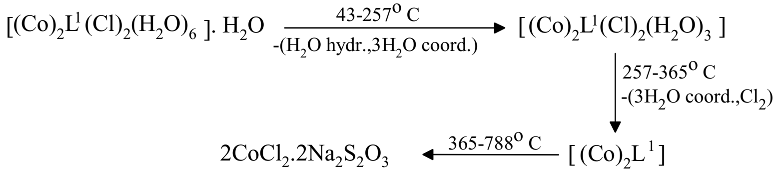

SCHEME 2

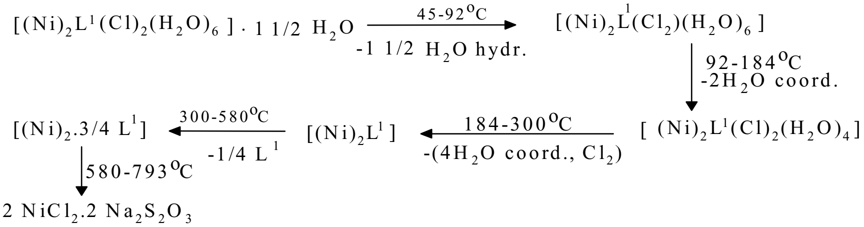

SCHEME 3

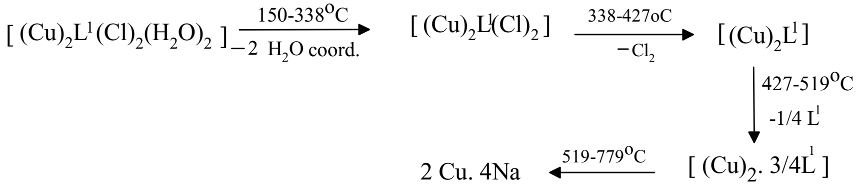

SCHEME 4

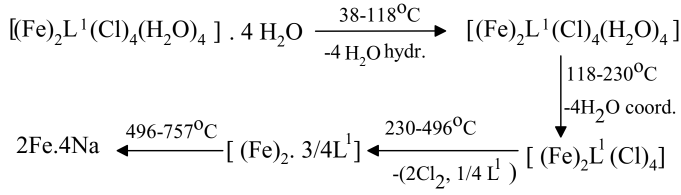

SCHEME 5

Kinetic Study

The activation energy (ΔE^*) values of the various decomposition stages for the metal complexes were determined from the TG and DTG themograms using the Coats–Redfern equation in the following form:

$$\log\left[\frac{\log\{W_f/(W_f - W)\}}{T^2}\right] = \log\left[\frac{AR}{\theta E^*}\left(1 - \frac{2RT}{E^*}\right)\right] - \frac{E^*}{2.303RT}$$

where W_f is the mass loss at the completion of the reaction, W is the mass loss up to temperature T, R is the gas constant, E is the activation energy, θ is the heating rate and $(1\text{–}(2RT/E^*)) \cong 1$. A plot of the left-hand side of this equation against 1/T gives a slope; from the intercept and linear slope of such stages, the (A) and (E^*) values were determined. The other kinetic parameters—the entropy of activation (ΔS^*), enthalpy of activation (ΔH^*), and the free energy change of activation (ΔG^*)—were calculated using the following relationships:

$$\Delta H^* = E - RT\,;\ \Delta G^* = H^* - TS^* \text{ and } \Delta S^* = 2.303\left(\log\frac{Ah}{KT}\right)R$$

where k and h are the Boltzmann and Planck constants, respectively. The negative values of entropy indicate that the activated complexes have more ordered systems than the reactants.

Antibacterial and Antifungal Assay

The screening data obtained for the compounds under study against the sensitive organisms *S. aureus*, *S. pyogenes*, *P. fluorescens*, *P. phaseolicola*, *F. oxysporum*, *A. fumigatus*, and *C. albicans* using the disc–agar diffusion technique[22] are summarized in Table VIII. A comparison of all tested compounds towards the different organisms brings out the following facts to light:

- The highest antimicrobial activity among the group of the tested compounds was observed against the fungi strains.
- The cyclodiphosph(V)azane ligand (**H_2L^1**) displayed intermediate activity against all types of bacteria and fungi species.
- Generally the activity of the free ligand was increased upon complexation with metal ions; this enhancement in activity can be explained

TABLE VIII Antimicrobial Screening Results of the Compounds Under Study

Compd. No.	Gram-positive bacteria		Gram-negative bacteria		Fungi		
H^2L_1	(36) 14	(37) 14	(44) 15	(41) 15	17 (49)	19 (48)	18 (50)
1	(38) 15	(50) 19	18 (53)	16 (43)	21 (60)	22 (55)	23 (64)
2	15 (38)	(47) 18	17 (50)	16 (43)	21 (60)	24 (60)	24 (67)
3	15 (38)	(47) 18	19 (56)	19 (51)	22 (63)	21 (53)	23 (64)
4	15 (38)	(39) 15	18 (53)	17 (56)	22 (63)	23 (58)	24 (92)
5	(64) 25	(67) 26	30 (88)	29 (78)	33 (94)	36 (90)	34 (94)
$MnCl_2 \cdot 4H_2O$	(26) 10	(29) 11	(35) 12	(30) 11	(46) 16	(35) 14	(36) 13
$CoCl_2 \cdot 6H_2O$	(49) 19	(50) 19	(44) 15	(27) 10	(46) 16	(40) 16	(50) 18
$NiCl_2 \cdot 6H_2O$	14 (36)	18 (47)	18 (53)	13 (35)	(37) 13	(45) 18	(31) 11
$CuCl_2 \cdot 2H_2O$	18 (46)	16 (42)	17 (50)	14 (38)	(43) 15	(35) 14	(33) 12
$FeCl_3 \cdot 6H_2O$	20 (51)	18 (47)	20 (59)	21 (57)	(57) 20	(48) 19	(61) 22
R.S.	39 (100)	38 (100)	34 (100)	37 (100)	35 (100)	40 (100)	36 (100)

- The test was done using the agar–disc diffusion method.
- % Activity index in parentheses.
- R.S., Reference standard: Chloramphencol, Cephalothin, and Cycloheximide were used as standard references for Gram-positive bacteria, Gram-negative bacteria, and antifungal, respectively.
- Inhibition values: –No effect; 3–13 low activity; 14–24 intermediate activity; 25–32 high activity; and >32 very high activity.

on the basis of chelation theory.[30] Chelation reduces the polarity of the metal ion considerably, mainly because of the partial sharing of its positive charge with donor groups and the possible π-electrons delocalization over the whole chelate ring. Chelation not only reduces the polarity of metal ion, but also increases the lipophilic character of the chelate. As a result of this, the interaction between the metal ion and the cell walls is favored, resulting in interference with normal cell processes.

- The effect of all metal complexes towards the fungi species was greater than the bacteria species.
- The metal complexes (**1–4**) displayed intermediate activity against all types of bacteria and fungi species with inhibition zone values greater than the free ligand ($\mathbf{H_2L^1}$).
- Fe(III) complex (**5**) had a higher degree of activity than all the other metal complexes or the free ligand ($\mathbf{H_2L^1}$) against all types of bacteria and fungi. It displayed high activity. Only the Fe(III) complex (**5**) had an effect comparable with that of the standards (Chloramphencol, Cephalothin, and Cycloheximide) towards the tested organisms. This may have been due to the trivalent state of the metal ion and/or the increase in the number of chloride around the metal ion.

STRUCTURAL INFORMATION

From all of the above observations based on elemental analysis, molar conductance, magnetic moment, and spectral (IR, ^{1}H-NMR, and UV-Vis) and thermal analyses, the proposed composition for the structure of the metal complexes (Figures 3 and 4) discussed herein indicates that the following:

- The ligand acts a dibasic tetradentate, and both the heterocyclic nitrogen and carbonyl oxygen atoms are involved in complexation with metal ions. Microanalysis reveals 2:1 metals-to-ligand ratio.
- All metal complexes are non-electrolyte. This implies the coordination of the chloride anions to the metal ion center.
- Octahedral structure was suggested for Mn(II), Co(II), Ni(II), and Fe(III) complexes. The Cu(II) complex is square planar.

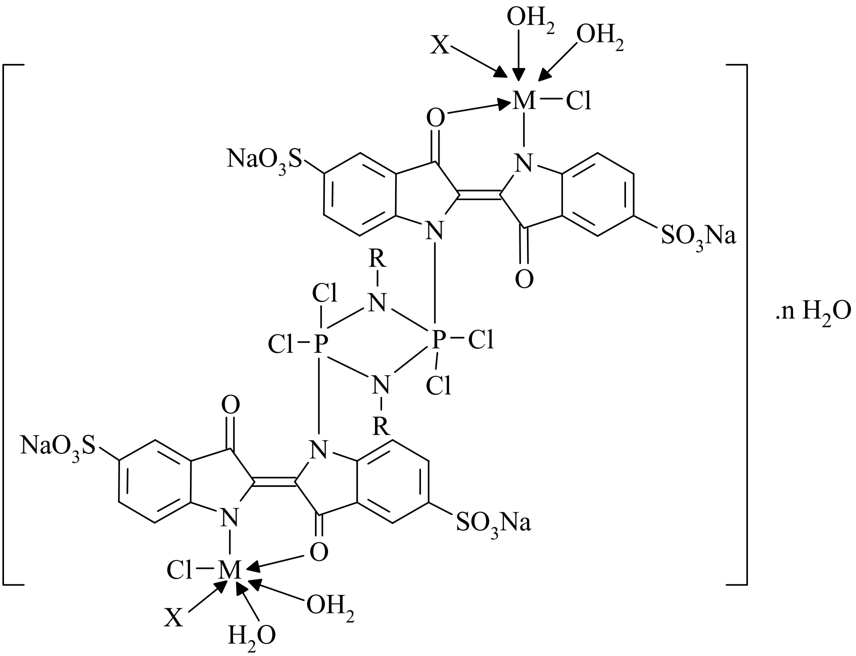

FIGURE 3 Suggested structure of the metal complexes **1–3** and **5**. M = Mn(II) or Co (II)$^-$: x = H_2O, n = 1; Ni(II): x = H_2O, n = 1.5; Fe(III): x = Cl, n = 4.

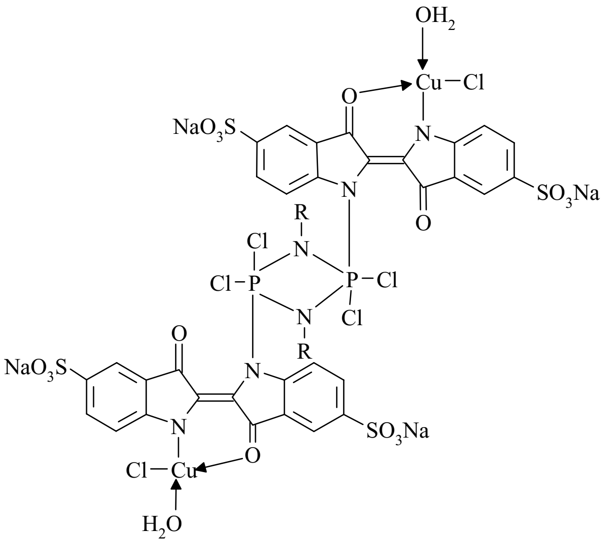

FIGURE 4 Suggested structure of the Cu(II) complex **4**.

REFERENCES

[1] A. A. M. Gad, G. M. H. Taha, A. E. Arifien, and M. Sh. Zoromba, *Phosphorus, Sulfur, and Silicon*, **182,** 2425 (2007).

[2] M. A. El-Nawawy, A. Z. Sayed, and Z. H. Abd El-Wahab, *Acta Pharm.*, **48,** 29 (1998).

[3] I. M. Aladzheva, O. V. Bykhovskaya, D. I. Lobanov, P. V. Petrovskii, K. A. Lysenko, and T. A. Mastryukova, *Chem. Heterocycl. Comp.*, **38,** 95 (2002).

[4] G. G. Mohamed, *Phosphorus, Sulfur, and Silicon*, **180,** 1569 (2005).

[5] K. V. Axenov, M. Leskel, and T. Repo, *J. Catalysis*, **238,** 196 (2006).

[6] I. M. Abd-Ellah, B. A. El-Sayed, M. A. El-Nawawy, and A. M. A. Alaghaz, *Phosphorus, Sulfur, and Silicon*, **177,** 2895 (2002).

[7] T. H. Afifi, M. A. El-Nawawy, Z. H. Abd El-Wahab, and H. A. Mahdy, *Phosphorus, Sulfur, and Silicon*, **132,** 101 (1998).

[8] I. M. Abd-Ellah, Y. Al-Shaibi, A. A. Issa, and M. S. El-Hammadi, *Phosphorus, Sulfur, and Silicon*, **139,** 29 (1998).

[9] H. N. Hassan, M. A. El-Nawawy, Z. H. Abd El-Wahab, and S. A. M. Shedid, *J. Indian Chem. Soc.*, **75,** 377 (1998).

[10] I. M. Abd-Ellah, A. A. Salman, R. S. Farag, and Z. H. Abd El-Wahab, *Pak. J. Sci. Res.*, **32,** 579 (1989).

[11] A. A. Salman, I. M. Abd-Ellah, A. N. El-Khazandar, and Z. H. Abd El-Wahab, *Phosphorus, Sulfur, and Silicon*, **40,** 9 (1988).

[12] E. Ibrahim, I. M. Abd-Ellah, L. S. Shaw, and I. Alnaimi, *Phosphorus, Sulfur, and Silicon*, **33,** 109 (1987).

[13] M. Abd-Ellah, E. H. M. Ebrahim, and A. N. El-Khazandar, *Phosphorus, Sulfur, and Silicon*, **31,** 13 (1987).

[14] I. M. Abd-Ellah, E. H. M. Ebrahim, and A. N. El-Khazandar, *Phosphorus, Sulfur, and Silicon*, **29,** 239 (1987).

[15] Z. H.Abd El-Wahab, *Ph.D.Thesis*, Al-Azhar University, Cairo, Egypt, 1992.

[16] Z. H. Abd El-Wahab, *M.Sc.Thesis,* Al-Azhar University, Cairo, Egypt, 1988.

[17] M. I. G. M. G. Travasso, P. C. S. Santos, A. M. F. O. Campos, M. M. M. Raposo, and N. Prasitpan, *Adv. Col. Sci. Technol.*, **6,** 95 (2003).

[18] I. Othman, R. M. Mohamed, I. A. Ibrahim, and M. M. Mohamed, *Appl. Catal.*, **A 299,** 95 (2006).

[19] A. H. Gemeay, I. A. Mansour, R. G. El-Sharkawy, and A. B.Zaki, *J. Mol. Catal.*, **A 19,** 109 (2003).

[20] I. T. Shadi, B. Z. Chowdhary, M. J. Snowden, and R. Withnall, *Spectrochim. Acta*, **A 59,** 2201 (2003).

[21] J. Bassett, R. C. Denney, G. H. Jeffery, and J. Mendham, *Vogel's Textbook of Quantitative Inorganic Analysis*, 4th= Ed.; Longmans, London, 1978.

[22] U. N. Tripathi, M. S. Ahmad, G. Venubabu, and P. Ramakrishna, *J. Coord. Chem.,* **60,** 1709 (2007).

[23] C. J. Cooksey, *Molecules*, **6,** 736 (2001).

[24] Z. H. Abd El-Wahab, *Spectrochim. Acta*, **A 67,** 25 (2007).

[25] M. M. Mashaly, Z. H. Abd El-Wahab, and A. A. Faheim, *J. Chin. Chem. Soc.*, **51,** 901 (2004).

[26] K. A. R. Salib, A. A. Saleh, S. Abu El-Wafa, and H. F. O. El-Shafiy, *J. Coord. Chem.*, **56,** 283 (2003).

[27] Z. H. Abd El-Wahab and M. R. El-Sarrag, *Spectrochim. Acta*, **A 60,** 271 (2004).

[28] T. M. A. Ismail, *J. Coord. Chem.*, **59,** 255 (2006).

[29] A. Z. El-Sonbati, A. A. M. Belal, S. I. El-Wakeel, and M. A. Hussien, *Spectrochim. Acta*, **A 60,** 965 (2004).

[30] B. Murukan and K. Mohanan, *J. Enz. Inhib. Med. Chem.* **22,** 65 (2007).